Shear-Tomography of clusters of galaxies

M. Lerchster[1], S. Seitz[1], R. Bender[1,2], H. Böhringer[2], P. Schneider[3]

[1] University Observatory Munich (USM), Munich
[2] Max Planck Institute for Extraterrestrial Physics (MPE), Garching
[3] Argelander-Institute of astronomy (AIfA), Bonn

ABSTRACT AND GOALS

The **shear tomography method** which shall be further developed with this work is potentially the cleanest one to constrain the **equation of state of dark energy** (EOS). We want to measure a photometric redshift-dependent shear signal behind **5 massive clusters** at redshifts of z ~ 0.25.
It is our goal to develop optimized optical colour criteria for sorting galaxies into groups with the same lensing strength.
The selected clusters are X-ray luminous, partly act as strong lenses and have lots of spectroscopic data to calibrate the photometric redshifts.

1. Probing dark energy

The presence of dark energy can be seen in the expansion history of the universe and its impact on structure formation. Clean ways to measure the expansion of the universe is to use **luminosity distances of supernovae** (assuming standard candle nature), **baryonic acoustic oscillations** as standard rods or **gravitational lensing** strength ratios. The latter method uses the fact that the gravitational shear of galaxies lensed by foreground clusters depends on a product of cluster properties and diameter distance ratios. If one compares the shear of galaxies within different redshift bins the cluster properties cancel out, and the shear ratio depends solely on the expansion history of the universe.

This so called **tomography method** is described in, e.g. Jain & Taylor (2003). The ratio of shears has a purely geometric dependence,
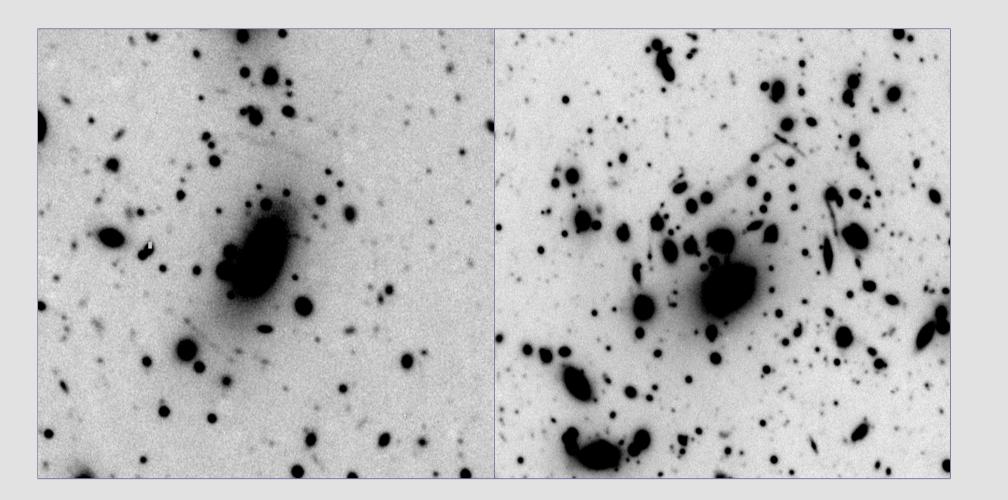
$$R(\Omega_V, \Omega_m, w) = \frac{\gamma(\chi_1, \chi_L)}{\gamma(\chi_2, \chi_L)}$$

$$\langle R \rangle = \frac{r(\chi_2)[r(\chi_1) - r(\chi_L)]}{r(\chi_1)[r(\chi_2) - r(\chi_L)]},$$

where χ is the comoving distance and $r(\chi)$ is the comoving angular diameter distance, that means it depends only on the global geometry of the Universe: Ω_V, Ω_m, w

Fig.1. Shear tomography sketch.

2. Clusters of galaxies

We will investigate the redshift-dependent lensing strength by mapping the shear field and obtaining multi waveband data behind **five** massive z = 0.25 foreground clusters which are **REFLEX-clusters,** Böhringer et al. (2004).

One advantage of choosing these fields (beyond their X-ray luminosity, and their nature as strong lenses) is that a large number of redshifts have been aquired with **VIMOS** in an ESO large program (PI Böhringer) in these fields, so the photometric redshifts can be spectroscopically calibrated at the least for the bright objects.

Another point is that the imaging observations of that program (VIMOS) have high quality and can be taken for alternative shear estimates in the **R and I-band** (**seeing** of order **0.6 – 0.8"**).

Fig.2. Examples of the cluster of galaxies used for the study. Shown are the **arcs** around the cluster centre in the deep VIMOS R-band images (**2.88 ks** for **RXCJ0528.9 ‑ 3927** (left panel) and **5.76 ks** for **RXCJ2308.3 ‑ 0211** (right panel).

3. Photometric redshifts

We will use **U, B, V, R and I** broad-band data to obtain distances to the lensing clusters and sources with **photo-z,** Bender et al. (2002) . The deep U-band data can partly compensate the lack of NIR data to discriminate the 4000 A and the Lyman-alpha break.

Fig.3. Comparison of the photometric redshift against spectroscopic redshift on the FDF. See Gabasch et al. (2004) for a demonstration of the accuracy of photo-z.

Shear tomography requires in principle large number density of background galaxies and **accurate photo-z's**. However, before routine application developments have to be made that can circumvent the **accurate photo-z's**, by, e.g. selecting only sub-samples of galaxies for which redshifts can be assigned most accurately, or by using colours such that galaxies lie most likely in redshift bins with well defined diameter distance ratios (lensing strength). See Jain et al. (2006) for a version of colour tomography.

4. Data reduction and shape estimates

The data will be reduced with the **ASTRO-WISE** pipeline (http://www.astro-wise.org) and the **GaBoDS** pipeline, Erben et al.(2005).

Shape measurements and corrections for PSF-smearing and anisotropies are carried out with the **KSB-method**, Kaiser et al. (1995). See Erben et al. (2001) for accuracy of the shear measurements.
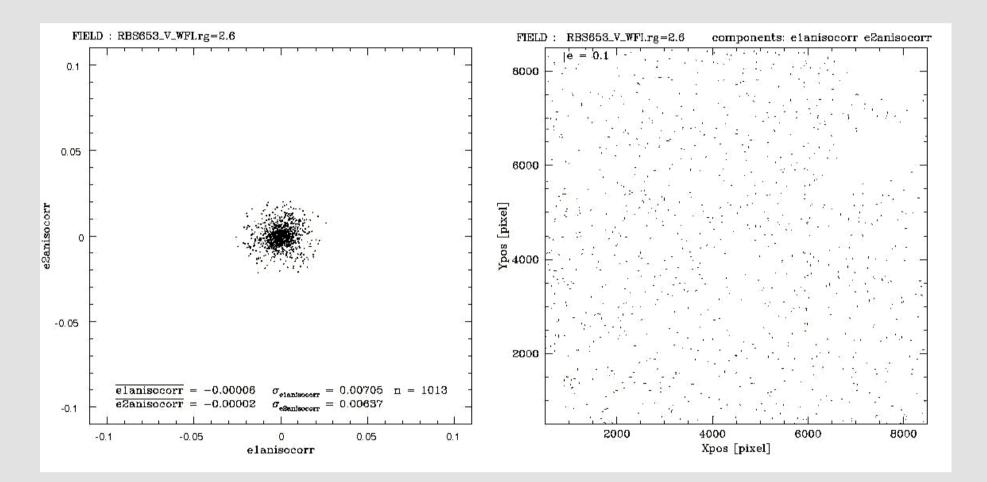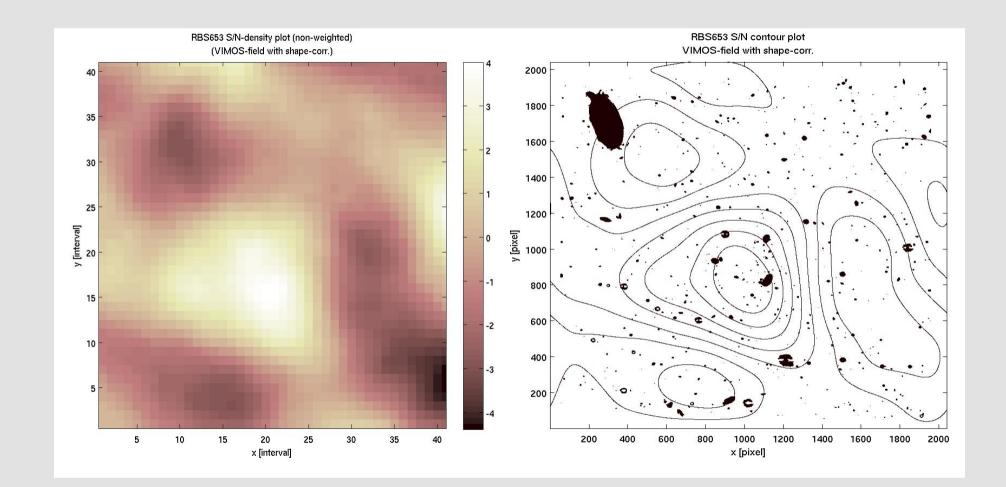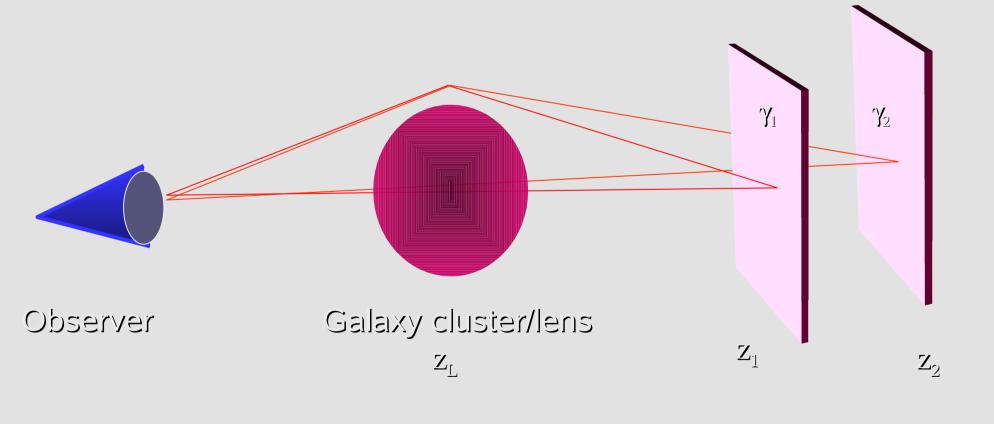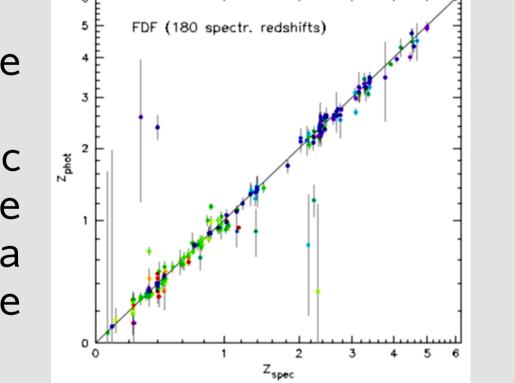

Fig.4. PSF anisotropy correction for the **RXCJ0528.9 ‑ 3927**. Left: **Ellipticity distribution** after subtraction of the polynomial fit. Right: **Stickplot** of the corrected ellipticities on the WFI V-band image FOV (34'x33').

Fig.5. First results of the weak lensing analysis of the cluster **RXCJ0528.9 ‑ 3927**. Left: **S/N-map** of the aperture mass on the grid. Right: **S/N-contour plot** as an overlay on the VIMOS R-band image FOV (8.04'x6.46').

5. Acknowledgements

6. References

Bartelmann M., Schneider P., 2001, Phys.Rept., 340
Bender R. et al., 2002, Ap&SS, 281, 539
Böhringer H. et al., 2004, A&A, 425, 367
Erben T., 2000, Ph.D. thesis, LMU
Erben T., P. Schneider, 2001, A&A, 366, 717
Erben T. et al., 2005, AN, 326, 432
Gabasch A., Bender R., Seitz S., 2004, A&A, 421, 41
Jain B., Taylor A., 2003, PhRvL9,302
Jain B., Connolly A., Takada M., 2006, arXiv: astro-ph/0609338
Kaiser N., Squires G., Broadhurst T., 1995, ApJ, 449, 460
Kausch W., Gitti M., Erben T., Schindler S., 2006, A&A, in prep.
Schneider P., 2006, glsw.conf, 269
van Waerbeke L., Mellier Y., Scheider P., 2001, A&A, 374, 757
Zhang Y.-Y., Böhringer H., 2006, A&A, 456, 55